

Seasonal Modulation of Tropical Cyclone Occurrence Associated with Coherent Indo-Pacific Variability during Decaying Phase of El Niño

Hiroaki UEDA

Faculty of Life and Environmental Sciences, University of Tsukuba, Tsukuba, Japan

Kana MIWA

Graduate School of Life and Environmental Sciences, University of Tsukuba, Tsukuba, Japan

and

Youichi KAMAE

Faculty of Life and Environmental Sciences, University of Tsukuba, Tsukuba, Japan

(Manuscript received 27 September 2017, in final form 23 April 2018)

Abstract

In this paper, the response of tropical cyclone (TC) activity to El Niño-Southern Oscillation (ENSO) and coherent sea surface temperature anomaly (SSTA) in the Indian Ocean (IO) is investigated, with a particular focus on the decaying phase of El Niño. The TC anomalies are obtained from the database for Policy Decision making for Future climate change (d4PDF). This dataset is based on 100-member ensemble simulations for the period of 1951–2010 using the state-of-the-art atmospheric general circulation model (AGCM) forced with the observed SST as well as the historical radiative forcing. The AGCM utilized in the d4PDF is the Meteorological Research Institute Atmospheric General Circulation Model (MRI-AGCM) with about 60 km horizontal resolution. Our analysis revealed a prolonged decrease in TC frequency (TCF) over the tropical Western Pacific during the post-El Niño years until the boreal fall. Dominance of anomalous anticyclone (AAC) over the Western Pacific induced by the delayed warming in the tropical IO is the main factor for the suppressed TC activity rather than the local SST change. In contrast, the TC number over the South China Sea tends to increase during the post-El Niño fall (September to November). The physical reason can be ascribed to the weakening of the AAC associated with the termination of IO warming. Thus, we demonstrate that the effect of the IO warming should be taken into account when the ENSO is considered as an environmental factor for predicting TC activity.

Keywords typhoon; Indian Ocean warming; capacitor effect; El Niño

1. Introduction

The western North Pacific (WNP) is the most active basin for tropical cyclone (TC) activity, accounting for more than one-third of global TCs (Chan 2005). Not only are TCs great contributors to climatological rainfall (Rodgers et al. 2000), but also their interannual variations have a massive socioeconomic influence on the world's most populated regions by landfall (Zhang

Corresponding author: Hiroaki Ueda, Life and Environmental Sciences, University of Tsukuba, 1-1-1 Tennoudai, Tsukuba, Ibaraki 305-8572, Japan
E-mail: ueda.hiroaki.gm@u.tsukuba.ac.jp
J-stage Advance Published Date: 14 May 2018

et al. 2009; Kumazawa et al. 2016). El Niño-Southern Oscillation (ENSO) is the first candidate for the modulation of WNP TCs through changing large-scale atmospheric as well as oceanic conditions. Previous studies identified that the annual TC number over the WNP does not have a significant relationship with ENSO (Lander 1994; Camargo and Sobel 2005), while the location of TC genesis shows southeastward displacement close to the dateline and the equator during the mature stage of El Niño compared to the La Niña years (Wang and Chan 2002; Kim et al. 2011). The El Niño-caused warmer sea surface temperature anomaly (SSTA) extending to the dateline is responsible for the longer lifetime of TCs, which often gives rise to higher intensities (Camargo and Sobel 2005).

The important role of ENSO in the regulation of TC frequency (TCF) over the WNP is primarily caused by a modulation of the Walker circulation rather than the local SSTA (Chan et al. 1985). During El Niño years, a weakened Walker circulation around the equatorial region, characterized by an anomalous upward (downward) motion over the Central (Western) Pacific, tends to suppress convection over and around the WNP and, hence, TC activity. It is further suggested that the large-scale environmental flow affects the genesis of TC through the modulation of vertical wind shear (Gray 1984) together with the extension of monsoon troughs (Chen et al. 1998). A decrease in the vertical wind shear caused by the attenuated Walker circulation during El Niño years allows TCs to occur eastward close to the dateline (Camargo et al. 2007a; Zhan et al. 2011a, b; Tao et al. 2012). The tracks of TCs over the WNP can be categorized into two groups: northward recurving passage toward Japan and landfall over Southern China by westward straight moving (Camargo et al. 2007b). In relation to the eastward shift of TC genesis during El Niño years, TCs are likely to recurve higher latitude (Elsner and Liu 2003; Fudeyasu et al. 2006). In contrast, TCs exhibit a little change in latitude during La Niña years, which moves toward Southern China, passing over the South China Sea.

A rich background literature can be found for the past 20 years regarding ENSO's influence over the Indian Ocean (IO hereafter) (e.g., Xie et al. 2009). The modulated Walker circulation anchored by the mature stage of El Niño (December to February) gives rise to delayed warming of tropical IO, which peaks in spring and persists through summer. Hereafter, seasons refer to those for the Northern Hemisphere. Ocean waves, such as the downwelling Rossby wave in the South IO (Xie et al. 2002) and warm Kelvin wave along the

equator (Ueda and Matsumoto 2000), as well as heat flux changes over the basin (Du et al. 2009; Klein et al. 1999), are the dominant agents in the basin-wide warming of the IO. Consequently, convections over the tropical IO become enhanced, which in turn reinforce the NWP anticyclone through atmospheric Kelvin wave adjustment (Annamalai et al. 2005; Ueda et al. 2015) besides the local air-sea coupling (Wang et al. 2000). This asymmetric response to the IO warming across the equator could be attributed to strong convection-circulation feedback emerging over the WNP during the boreal summer. Using the linear baroclinic model, Xie et al. (2009) confirmed that diabatic cooling over the WNP relevant to the suppressed convection preferentially amplifies the AAC intensity to the east of the Philippines through the convective feedback. Those trans-basin interactions are collectively called the "Indo-western Pacific Ocean Capacitor (IPOC) effect" (Xie et al. 2016).

The notion of IPOC's impacts on the NWP TC occurrences via the intensification of NWP anticyclone and increase in the magnitude of vertical shear is more relevant for explaining the decrease of the TC number despite a little change in the local SST. It has been revealed that the warmed tropical IO can account for as much as 50 % of the variance in the decrease of TC frequencies over the NWP during summer after the peak El Niño season (Du et al. 2011; Zhan et al. 2011, Kosaka et al. 2013). Those observational studies were confirmed by sensitivity experiments using the air-sea coupled model (Takaya et al. 2017), implicating the development of seasonal TC predictions.

Although the abovementioned observational evidence and modeling studies have greatly advanced our understanding of the TC behaviors influenced by the planetary-scale environmental flow associated with patterns of SST in the Indo-Pacific domain, it can still be meaningful to reduce uncertainty which comes from both of the limited TC samples. In addition to this, Wu et al. (2012) demonstrated that the initial conditions and internal variability in the model are an important factor in TC activities. Thus, we took advantage of high-resolution AGCM (60 km) ensemble simulations (100 members) forced with the observed SST (1951–2010), which allowed the evaluation of the statistical significance. This paper is organized as follows. Section 2 describes the observational data and the AGCM experiment. Section 3 discusses to what extent and what properties of TC activity relate to environmental flow anchored to the underlying SSTA in the tropical Indo-Pacific Ocean. A summary is given in Section 4.

2. Data and method

We used 100-ensemble historical simulations that were obtained from the database for Policy Decision making for Future climate change (d4PDF). The model utilized in the d4PDF is the Meteorological Research Institute Atmospheric General Circulation Model (MRI-AGCM) version 3.2 (Mizuta et al. 2012), which is a spectral model with triangular truncation at total wave number 319 (T319; equivalent to 60 km horizontal resolution) and 64 levels in the vertical direction. The simulation was run for the period of 1951–2010 forced with the observed monthly-mean SST and sea ice (Hirahara et al. 2014) together with historical radiative forcing. Small perturbations, constructed from major modes of the interannual variation of SST, are added to the observed SST named Centennial Observation Based Estimates of SST version 2 (COBE-SST2; Hirahara et al. 2014). For more details, readers are referred to Mizuta et al. (2017). Identification of TCs in the d4PDF is based on a detection method that was firstly developed by Oouchi et al. (2006) and modified by Murakami et al. (2012). The meteorological elements adopted in this study are the maximum wind speed at 850 hPa (greater than 13 m s^{-1}) together with relative vorticity (greater than 8.0×10^{-5}), difference of warm core temperature at 300, 500, and 700 hPa exceeding those in the surrounding region by 0.8°C , vertical wind shear (the horizontal wind speed at 850 hPa is greater than at 300 hPa), and duration (longer than 36 hours). In the present study, the TCF is computed at six-hour intervals (Yoshida et al. 2017).

The best track data of TCs are from the Unisys Weather Hurricane/Tropical Data website (Unisys 2015) provided by the Joint Typhoon Warning Center (JTWC) and the National Hurricane Center (NHC), which includes the position and intensity of the observed TCs at six-hour intervals. TCs are defined as having a maximum surface wind speed in a closed cyclonic circulation greater than 18 m s^{-1} (35 knots). Readers are referred to Murakami et al. (2012) for more details. We investigated the TC activity for the period starting from 1979 when the satellite data were operationally used so that failure of detection would be reduced (Webster et al. 2005; Emanuel 2007). Reference data for geopotential heights are taken from the Japanese 55-year Reanalysis (JRA-55) (Kobayashi et al. 2015). In the present paper, we focused on the three major El Niño events of 1987/88, 1997/98, and 2009/2010 in order to study how local as well as remote SST anomalies affect TC activity.

3. Results

3.1 SSTA and environmental flow

A spatial pattern of SSTA in the Indo-Pacific domain affects the large-scale environmental flow and thus the TC characteristics, including the location of TC genesis and TC tracks. Regarding the extent to which our three targeted ENSO events resemble the IPOC (Xie et al. 2016), we show in Figs. 1a–c the composite characteristics of seasonal evolution of the observed SST and atmospheric circulation during the decaying phase of El Niño. DJFM season (Fig. 1a) includes the peak phase of El Niño and IO warming, which are recognizable as positive SSTA in the broad IO and negative SSTA in the tropical Western Pacific. A positive geopotential anomaly, which is indicative of anomalous anticyclonic circulation (AAC hereafter), emerges to the northeast of the Philippines. The Kelvin wave-induced Ekman divergence caused by the remote IO warming accounts for the intensification of the Pacific anticyclone besides the effect of the local negative SSTA. Xie et al. (2009) indicated that the reason for the intensification of the AAC is closely related to the presence of active convection over NWP during the boreal summer, where the convection-circulation feedback preferentially amplifies the intensity of the AAC.

Wang et al. (2000) proposed that the AAC causes a decrease in SST on the southeastern flank by enhancing the climatological northeast trade winds. The cold SSTA suppresses convective activity aloft, reinforcing the anticyclone with an atmospheric Rossby response. During AMJJ season (Fig. 1b), the SSTA in the tropical Western Pacific to the west of 150°E changes from negative to positive, whereas those around the dateline turn to be negative, indicating the transition from El Niño to La Niña. The spatial pattern and sign of SSTA continue to the next ASON season (Fig. 1c) toward the mature stage of La Niña with increasing amplitude. Note that the AAC can still be found in AMJJ to the east of the Philippines in spite of the underlying positive SSTA, which is consistent with the warm SSTA in the IO and its remote impact (Annamalai et al. 2005; Ueda et al. 2015). The AAC slightly retreats northeastward through the ASON. Meanwhile, the geopotential height in the Eastern IO tends to have an opposite sign in comparison with those in the half year before. In order to confirm the model's performance in the d4PDF, we examined the composite anomalies for geopotential height and precipitation (Figs. 1d–f). Overall, El Niño-related anomalies are well simulated in the d4PDF run. However, biases are apparent in the

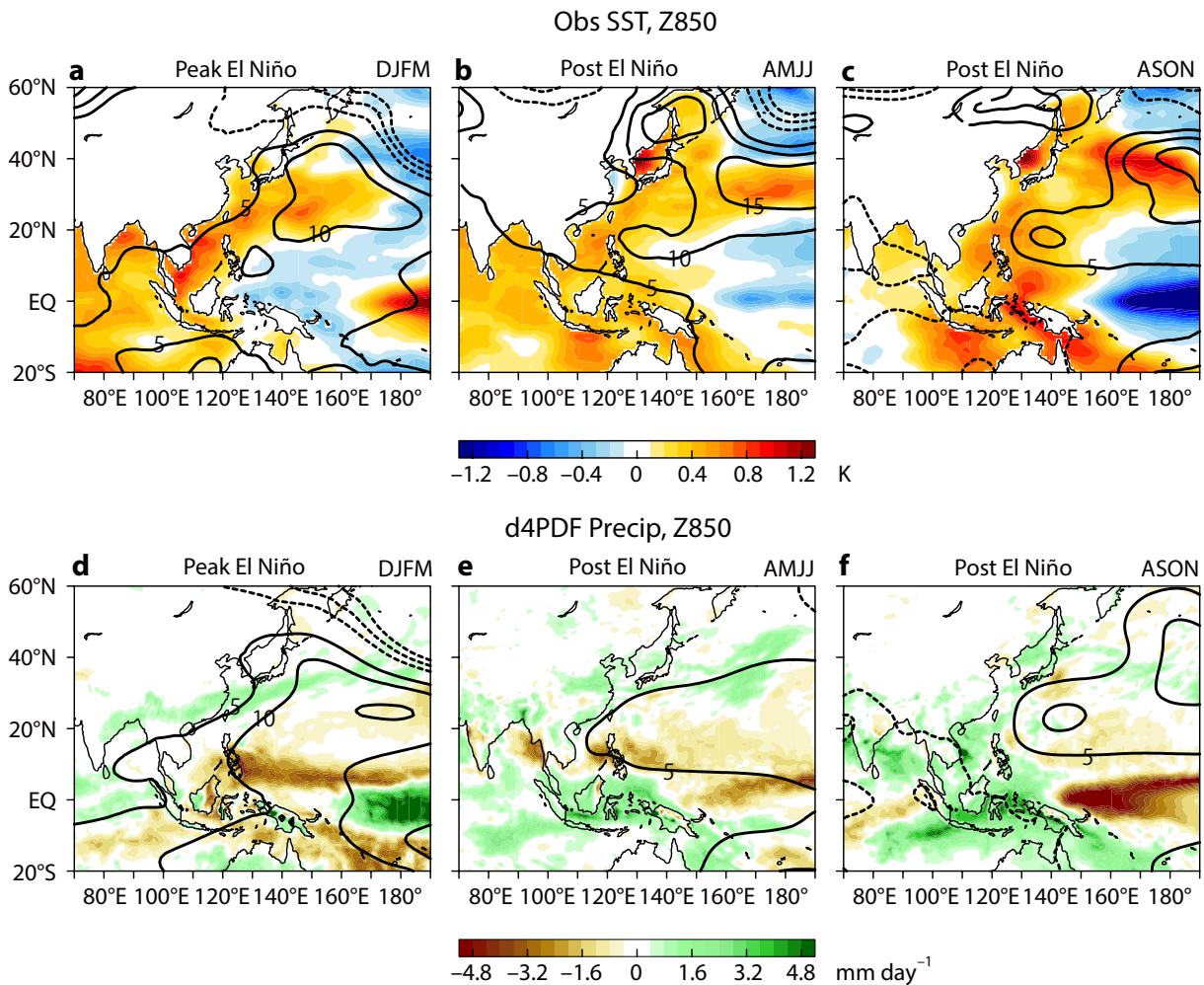


Fig. 1. Composite anomalies of the observed COBE-SST2 (shading; K) and 850 hPa geopotential height (contours; m) during post-El Niño years (1988, 1998, and 2010) from the climatological mean (1979–2010) for the (a) DJFM, (b) AMJJ, and (c) ASON seasons. (d), (e), and (f) are the same as (a), (b), and (c), but for precipitation (shading; mm day^{-1}) in the d4PDF ensemble.

AMJJ season (Fig. 1e). The simulated AAC tends to be weaker than the observations especially over the midlatitude WNP. In comparison with the observed precipitation anomalies (Fig. 2), no negative rainfall anomaly over the Indochina Peninsula was clearly found in the simulation, which is consistent with the weaker geopotential height anomaly over this region (Fig. 1e).

3.2 Locations and frequency of TCs

Figure 3 displays the TCF during the latter half of the calendar year (July to December) for El Niño and the post-El Niño years based on d4PDF (shading) and

the best track data (open circles). The climatology of d4PDF (contour) shows two maxima appearing in the South China Sea and the Western Pacific across the Philippines. Compared with the post-El Niño years, the TCF during El Niño obtained from not only the d4PDF but also the best track data shows a distinct southeastward shift toward the dateline, confirming the previous studies (Wang and Chan 2002; Kim et al. 2011).

Contours in Fig. 4 show the long-term mean of TCF based on the best track data (upper panels) and the d4PDF (lower panels). Climatologically, TCs in both observation and d4PDF develop in the vicinity

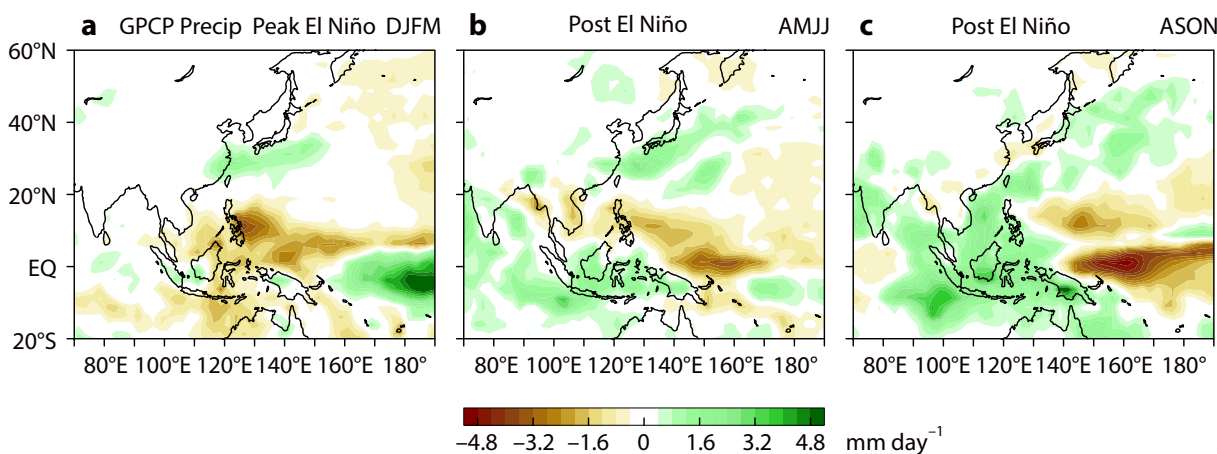


Fig. 2. Composite anomalies of the observed precipitation (mm day^{-1}) taken from the Global Precipitation Climatology Project (GPCP; Adler et al. 2003) during post-El Niño years (1988, 1998, and 2010) from the climatological mean (1979–2010) for the (a) DJFM, (b) AMJJ, and (c) ASON seasons.

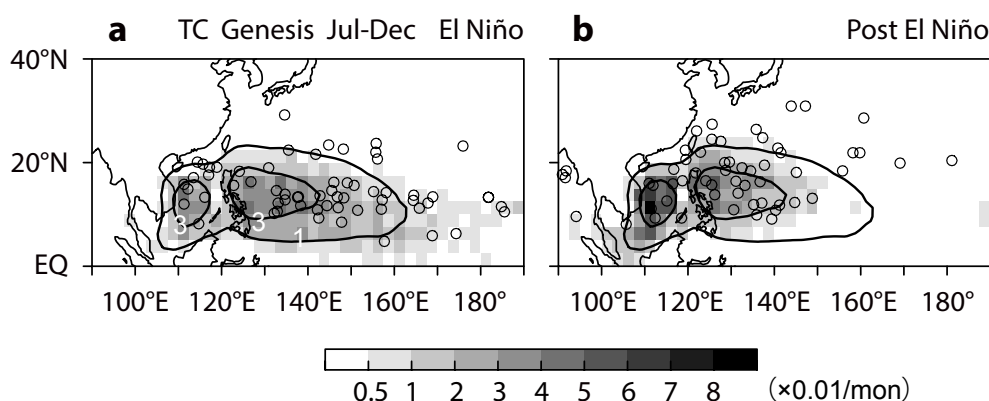


Fig. 3. TCF based on d4PDF (shading; $\times 0.01 \text{ month}^{-1}$) for the season July to December during (a) El Niño years (1987, 1997, and 2009) and (b) post-El Niño years (1988, 1998, and 2010) together with its climatology (contours at 1 and 3 $\times 0.01 \text{ month}^{-1}$) calculated at each $2.5^\circ \times 2.5^\circ$ grid. The open circles denote the genesis locations of TCs obtained from the best track data.

of the Philippines during the winter, which moves northeastward as the season evolves. From a monsoon perspective, the eastward expansion of lower tropospheric westerlies between the spring and summer against the easterly trade wind creates a weak wind region over the confluence zone and results in high SSTs (Ueda and Yasunari 1996). Furthermore, the convergence of those large-scale flows enhances meridional wind shear and the ensuing increase in barotropic instability (Murakami and Matsumoto 1994). Those environmental conditions are consistent with the eastward extension of TC genesis associated with

the tropical disturbances (Takayabu and Nitta 1993). As for the interannual variation in the d4PDF, the TCF during DJFM (Fig. 4d) is suppressed over the South China Sea and Western Pacific to the west of 140°E , which is collocated with dominance of the AAC and underlying cold SSTA (see Fig. 1a). The persistent AAC over the Western Pacific during the succeeding AMJJ (Fig. 1b) can account for the decrease in the TCF around the Philippines (Fig. 4e). When it comes to ASON, corresponding to the later season of TC genesis, the TCF increases in the South China Sea, whereas the Western Pacific still exhibits a negative

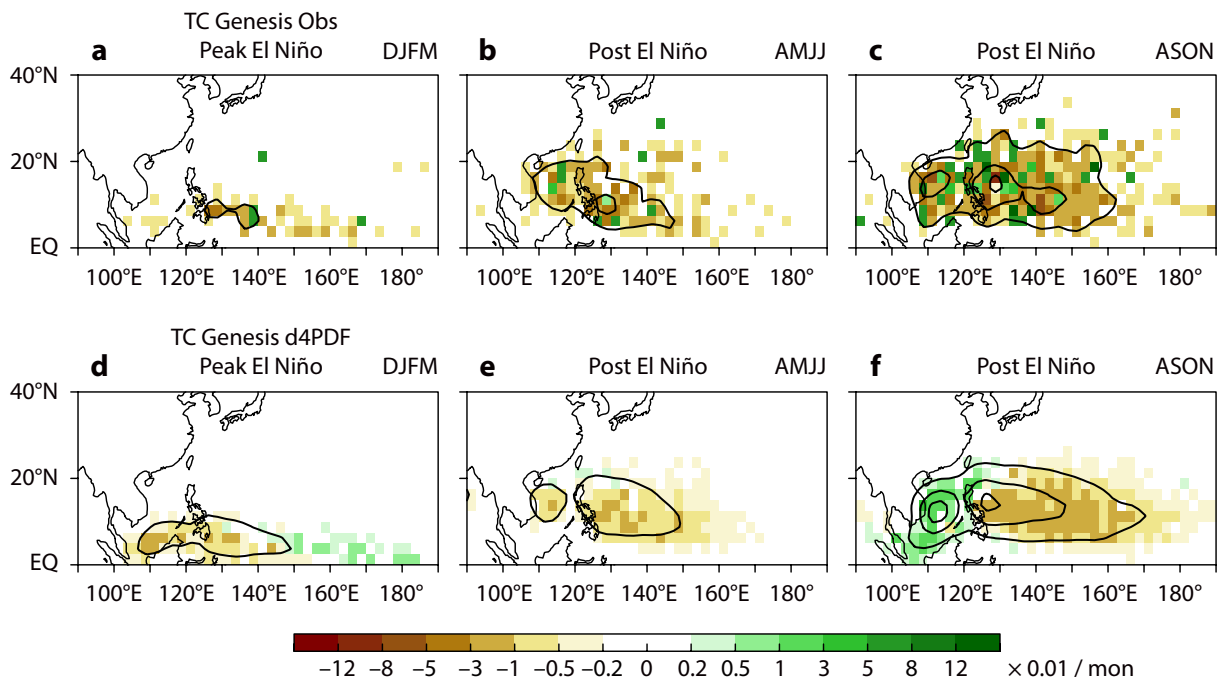


Fig. 4. Anomalies of TCF from the climatological mean (1979–2010) based on the best track data (shading; $\times 0.01 \text{ month}^{-1}$) during post-El Niño years (1988, 1998, and 2010) for the (a) DJFM, (b) AMJJ, and (c) ASON seasons. Contours (1, 3, and $5 \times 0.01 \text{ month}^{-1}$) show the TC climatology in each season. (d), (e), and (f) are the same as (a), (b), and (c), but for the d4PDF.

anomaly with enhancing signal. It is conceivable that termination of the IO warming and coherent weakening of subsidence associated with the atmospheric teleconnection contribute to the diminishment of AAC over the South China Sea, hence the increase in TCF. We will revisit this issue in the next subsection. Meanwhile, the Central-Eastern Pacific experiences a rapid transition from warming to cooling, which excites the descending Rossby waves to its northwest region and results in suppressed TCF through enhancement of the AAC (Wang et al. 2017). In comparison with the observational records of TCF anomalies, the model succeeded in reproducing a decrease in the TCF around the Philippines between December and July. During the ASON season, the observed decrease in the TCF between the dateline and the Philippines was also well simulated, whereas positive and negative anomalies seen in the observations coexisted in the South China Sea, showing a rather obscure spatial distribution, presenting the merit of using the d4PDF, which provides statistically significant signals based on the large ensemble members.

3.3 The South China Sea

We now focus more closely on the TCF in the South China Sea by comparing year-to-year differences. The climatology of TCF (Fig. 5a) indicates that the number of TCs tends to increase from June toward its peak in September, which gradually decreases until December. Fewer TCs are observable between January and June. Regarding the interannual variations (Fig. 5b), the TC count in El Niño decaying years of d4PDF (gray bar) is suppressed from December to August, but it suddenly turns positive toward the winter, except for September 2010. These TC anomalies are consistent with the IPOC's effect (Xie et al. 2016), namely, transition from El Niño to La Niña (blue line) followed by the delayed North IO warming (orange line). The Z850 anomalies averaged over the South China Sea (purple line in Fig. 5) show a decreasing tendency from August, which indicates weakening of suppressant effect for the TC activity. It has been pointed out that seasonal variability in TCF between the simulations and observations reaches its peak in August (Wu et al. 2012), which is consistent with the diminishment of the AAC from the late summer. The tendency of Z850 is coherent with the IO SST anoma-

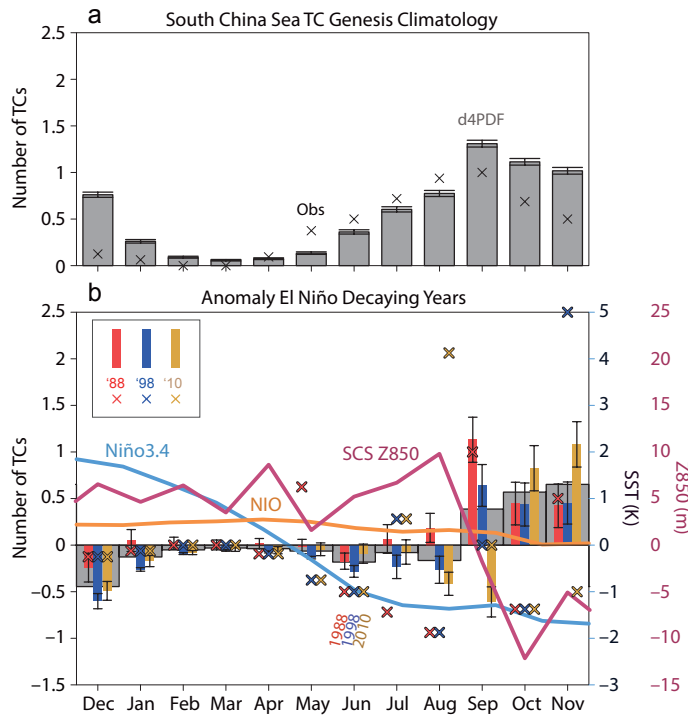


Fig. 5. Evolution of TC population in the South China Sea (0–25°N, 100–120°E) per month obtained from d4PDF (filled bars) and the best track data (cross marks). The error bars represent the 95 % confidence intervals derived from spreads among the 100 ensemble members. (a) Climatological mean (1979–2010) and (b) anomalies during the decaying phase of El Niño, focusing on typical events (1988, red; 1998, blue; 2010, yellow; three-year composite, gray). The blue/orange line shows the composite Niño3.4 (5°N–5°S, 170–120°W)/North IO (5–25°N, 40–100°E) SST anomaly (right axis; K) from the climatology (1979–2010). The purple line denotes geopotential height anomalies (m) in the JRA55 averaged over the South China Sea.

lies, implicating an important role of the IPOC’s effect in the SCS TCF. It should be noted here that the best track data during October 1988, 1998, and 2010 and November 2010 are not consistent with the simulated results. These gaps in the TCF between the AGCM runs in response to the prescribed SST anomalies and those in the observations might be attributed to the initial conditions or atmospheric internal variability (Wu et al. 2012). We confirmed that the observed TCF anomalies are within the maximum–minimum range of the model’s response, implicating some role of the internal variability of the atmosphere besides the model bias (Fig. 6).

It should be mentioned here that the model spreads become larger after July, showing less predictability relevant to the atmospheric internal variability. On the other hand, the present study indicates higher predictability during the suppressing stage of TC activity before June associated with the dominance of AAC

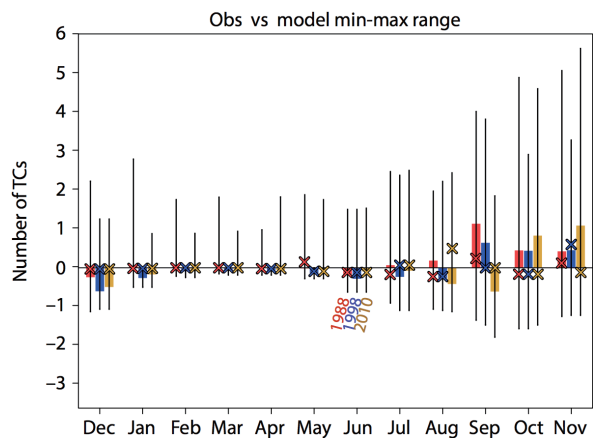


Fig. 6. Similar to Fig. 5b, but error bars indicate minimum–maximum ranges among 100 members of model simulations. Due to the large spreads among the members, the scale of the y-axis is different from that in Fig. 5b.

Table 1. Seasonal (four-month mean) anomalies of SST averaged over the Niño3.4 (5°N–5°S, 170–120°W) and North IO (5–25°N, 40–100°E) and TCF in the South China Sea. The 5 % level of statistical significance is shown in parentheses.

	DJFM	AMJJ	ASON
Niño3.4 (°C)			
Year 87/88	0.58	–1.3	–1.71
Year 97/98	2.29	–0.1	–1.29
Year 09/10	1.44	–0.27	–1.47
North Indian Ocean (°C)			
Year 87/88	0.38	0.09	0.02
Year 97/98	0.43	0.47	0.17
Year 09/10	0.6	0.72	0.29
d4PDF TCF (month ^{–1})			
Year 87/88	–0.043 (± 0.029)	–0.026 (± 0.029)	0.546 (± 0.056)
Year 97/98	–0.253 (± 0.011)	–0.181 (± 0.017)	0.316 (± 0.055)
Year 09/10	–0.195 (± 0.015)	–0.066 (± 0.022)	0.221 (± 0.050)
Best Track TCF (month ^{–1})			
Year 87/88	–0.047	–0.172	–0.031
Year 97/98	–0.047	–0.172	0.219
Year 09/10	–0.047	–0.172	0.219

in comparison with those in the enhancing phase after September.

The other caveat is that AGCM tends to exaggerate the SST anomalies by simulating a positive SST–convection relationship (Wang et al. 2005). As was already seen in the comparison of the geopotential height between the observations and the d4PDF (Figs. 1b, e), the intensity of AAC around the South China Sea was slightly weaker than the observation, which should be considered when we discuss the suppressant effect for TCF anchored with remote SST anomalies. Table 1 displays four-month mean anomalies of TC number with its statistical significance and the index of ENSO and IO-SSTA based on Fig. 5. Overall, these results show the coherent seasonal anomalies after the peak phase of El Niño except for AMMJ 1988. This is because of the earliest transition from El Niño to La Niña and the ensuing diminishment of the suppressant effect on TC activity anchored with the IO warming.

4. Conclusions

The influence of ENSO together with the basin-wide warming in the tropical IO on TC activity is analyzed, with a particular focus on the decaying phase of El Niño. In order to reduce the uncertainty resulting from the limited sample of the observed TC track, a huge ensemble (100 members) simulation forced by

the observed SST named “d4PDF” was utilized. In the present study, the causal relationship between the TCF and environmental changes in three typical El Niño events is examined. Our analysis reveals a sharp decrease in the TC number in the tropical Western Pacific during the post-El Niño years until the early winter. The dominance of AAC over the Western Pacific caused by the prolonged warming in the tropical IO is a crucial factor, rather than the local SSTA. In contrast, the South China Sea exhibits an opposing response during the post-El Niño season from September, showing a remarkable increase in the TC count. This can be ascribed to the weakening of subsidence anchored with the positive IO SST anomalies, which diminish in September.

Our study supports the preliminary finding about the combined effects of ENSO and related IO warming on TC anomalies (Du et al. 2011; Zhan et al. 2011a; Mei et al. 2015) by the use of a huge ensemble simulation, suggesting high predictability of seasonal TC occurrence. Recently, Zhan et al. (2013) revealed that the southward positive SST gradient between the Southwestern Pacific Ocean and the Western Pacific Ocean emerges during the decaying phase of El Niño, which is also an important factor for the decrease in TCF over the Western Pacific. It has been noted that the correlation between warming in the eastern IO

and TCF in the Western Pacific became large after the late 1970s (Zhan et al. 2014), which implicates that understanding the climate shift would help improve seasonal prediction skills for the TC activities. The prediction of TC activity remains a grand challenge for Southeast and East Asia. Future work such as passage of TCs and subsequent landfall will improve seasonal forecasts.

Acknowledgments

This study utilized the database for Policy Decision making for Future climate change (d4PDF), which was produced under the SOUSEI program and maintained by the DIAS server funded by the MEXT. The authors thank Dr. Kouhei Yoshida from the Meteorological Research Institute for providing the TC data. This work was also supported by JSPS KAKENHI grant number 17K01223, the Integrated Research Program for Advancing Climate Models (TOUGOU program) from the MEXT, Japan, and the industry-academia collaboration project of University of Tsukuba.

References

- Adler, R. F., G. J. Huffman, A. Chang, R. Ferraro, P.-P. Xie, J. Janowiak, B. Rudolf, U. Schneider, S. Curtis, D. Bolvin, A. Gruber, J. Susskind, P. Arkin, and E. Nelkin, 2003: The version-2 Global Precipitation Climatology Project (GPCP) monthly precipitation analysis (1979-present). *J. Hydrometeorol.*, **4**, 1147–1167.
- Annamalai, H., S.-P. Xie, J. P. McCreary, and R. Murtugudde, 2005: Impact of Indian Ocean sea surface temperature on developing El Niño. *J. Climate*, **18**, 302–319.
- Camargo, S. J., and A. H. Sobel, 2005: Western North Pacific tropical cyclone intensity and ENSO. *J. Climate*, **18**, 2996–3006.
- Camargo, S. J., K. A. Emanuel, and A. H. Sobel, 2007a: Use of a genesis potential index to diagnose ENSO effects on tropical cyclone genesis. *J. Climate*, **20**, 4819–4834.
- Camargo, S. J., A. W. Robertson, S. J. Gaffney, P. Smyth, and M. Ghil, 2007b: Cluster analysis of typhoon tracks. Part II: Large-scale circulation and ENSO. *J. Climate*, **20**, 3654–3676.
- Chan, J. C. L., 1985: Tropical cyclone activity in the northwest Pacific in relation to the El Niño/Southern Oscillation phenomenon. *Mon. Wea. Rev.*, **113**, 599–606.
- Chan, J. C. L., 2005: Interannual and interdecadal variations of tropical cyclone activity over the western North Pacific. *Meteor. Atmos. Phys.*, **89**, 143–152.
- Chen, T.-C., S.-P. Weng, N. Yamazaki, and S. Kiehn, 1998: Interannual variation in the tropical cyclone formation over the western North Pacific. *Mon. Wea. Rev.*, **126**, 1080–1090.
- Du, Y., S.-P. Xie, G. Huang, and K. Hu, 2009: Role of air-sea interaction in the long persistence of El Niño—Induced north Indian Ocean warming. *J. Climate*, **22**, 2023–2038.
- Du, Y., L. Yang, and S.-P. Xie, 2011: Tropical Indian Ocean influence on Northwest Pacific tropical cyclones in summer following strong El Niño. *J. Climate*, **24**, 315–322.
- Elsner, J. B., and K. B. Liu, 2003: Examining the ENSO typhoon hypothesis. *Climate Res.*, **25**, 43–54.
- Emanuel, K., 2007: Environmental factors affecting tropical cyclone power dissipation. *J. Climate*, **20**, 5497–5509.
- Fudeyasu, H., S. Iizuka, and T. Matsuura, 2006: Impact of ENSO on landfall characteristics of tropical cyclones over the western North Pacific during the summer monsoon season. *Geophys. Res. Lett.*, **33**, L21815, doi:10.1029/2006GL027449.
- Gray, W. M., 1984: Atlantic seasonal hurricane frequency. Part I: El Niño and 30 mb Quasi-Biennial oscillation influences. *Mon. Wea. Rev.*, **112**, 1649–1668.
- Hirahara, S., M. Ishii, and Y. Fukuda, 2014: Centennial-scale sea surface temperature analysis and its uncertainty. *J. Climate*, **27**, 57–75.
- Kim, H.-M., P. J. Webster, and J. A. Curry, 2011: Modulation of North Pacific tropical cyclone activity by three phases of ENSO. *J. Climate*, **24**, 1839–1849.
- Klein, S. A., B. J. Soden, and N.-C. Lau, 1999: Remote sea surface temperature variations during ENSO: Evidence for a tropical atmospheric bridge. *J. Climate*, **12**, 917–932.
- Kosaka, Y., S.-P. Xie, N.-C. Lau, and G. A. Vecchi, 2013: Origin of seasonal predictability for summer climate over the northwestern Pacific. *Proc. Natl. Acad. Sci. U.S.A.*, **110**, 7574–7579.
- Kobayashi, S., Y. Ota, Y. Harada, A. Ebata, M. Moriwa, H. Onoda, K. Onogi, H. Kamahori, C. Kobayashi, H. Endo, K. Miyaoka, and K. Takahashi, 2015: The JRA-55 Reanalysis: General specifications and basic characteristics. *J. Meteor. Soc. Japan*, **93**, 5–48.
- Kumazawa, R., H. Fudeyasu, and H. Kubota, 2016: Tropical cyclone landfall in Japan during 1900–2014. *Tenki*, **63**, 855–861 (in Japanese).
- Lander, M. A., 1994: An exploratory analysis of the relationship between tropical storm formation in the western North Pacific and ENSO. *Mon. Wea. Rev.*, **122**, 636–651.
- Mei, W., S.-P. Xie, M. Zhao, and Y. Wang, 2015: Forced and internal variability of tropical cyclone track density in the western North Pacific. *J. Climate*, **28**, 143–167.
- Mizuta, R., H. Yoshimura, H. Murakami, M. Matsueda, H. Endo, T. Ose, K. Kamiguchi, M. Hosaka, M. Sugi, S. Yukimoto, S. Kusunoki, and A. Kitoh, 2012: Climate simulations using MRI-AGCM3.2 with 20-km grid. *J. Meteor. Soc. Japan*, **90A**, 233–258.
- Mizuta, R., A. Murata, M. Ishii, H. Shioyama, K. Hibino, N. Mori, O. Arakawa, Y. Imada, K. Yoshida, T. Aoyagi, H. Kawase, M. Mori, Y. Okada, T. Shimura, T. Nagatomo, M. Ikeda, H. Endo, M. Nosaka, M. Arai, C. Takahashi, K. Tanaka, T. Takemi, Y. Tachikawa, K. Temur, Y. Kamae, M. Watanabe, H. Sasaki, A. Kitoh, I. Takayabu, E. Nakakita, and M. Kimoto, 2017: Over 5000 years of ensemble future climate simulations by 60-km global and 20-km regional atmospheric models.

- Bull. Amer. Meteor. Soc.*, **98**, 1383–1398.
- Murakami, H., R. Mizuta, and E. Shindo, 2012: Future changes in tropical cyclone activity projected by multi-physics and multi-SST ensemble experiments using the 60-km-mesh MRI-AGCM. *Climate Dyn.*, **39**, 2569–2584.
- Murakami, T., and J. Matsumoto, 1994: Summer monsoon over the Asian continent and western North Pacific. *J. Meteor. Soc. Japan*, **72**, 719–745.
- Oouchi, K., J. Yoshimura, H. Yoshimura, R. Mizuta, S. Kusunoki, and A. Noda, 2006: Tropical cyclone climatology in a global-warming climate as simulated in a 20 km-mesh global atmospheric model: Frequency and wind intensity analyses. *J. Meteor. Soc. Japan*, **84**, 259–276.
- Rodgers, E. B., R. F. Adler, and H. F. Pierce, 2000: Contribution of tropical cyclones to the North Pacific climatological rainfall as observed from satellites. *J. Appl. Meteor.*, **39**, 1658–1678.
- Takaya, Y., Y. Kubo, S. Maeda, and S. Hirahara, 2017: Prediction and attribution of quiescent tropical cyclone activity in the early summer of 2016: Case study of lingering effects by preceding strong El Niño events. *Atmos. Sci. Lett.*, **18**, 330–335.
- Takayabu, Y. N., and T. Nitta, 1993: 3–5 day-period disturbances coupled with convection over the tropical Pacific Ocean. *J. Meteor. Soc. Japan*, **71**, 221–246.
- Tao, L., L. Wu, Y. Wang, and J. Yang, 2012: Influences of tropical Indian Ocean warming and ENSO on tropical cyclone activity over the western North Pacific. *J. Meteor. Soc. Japan*, **90**, 127–144.
- Ueda, H., and T. Yasunari, 1996: Maturing process of summer monsoon over the western North Pacific: A coupled ocean/atmosphere system. *J. Meteor. Soc. Japan*, **74**, 493–508.
- Ueda, H., and J. Matsumoto, 2000: A possible triggering process of east-west asymmetric anomalies over the Indian Ocean in relation to 1997/98 El Niño. *J. Meteor. Soc. Japan*, **78**, 803–818.
- Ueda, H., Y. Kamae, M. Hayasaki, A. Kitoh, S. Watanabe, Y. Miki, and A. Kumai, 2015: Combined effects of recent Pacific cooling and Indian Ocean warming on the Asian monsoon. *Nat. Commun.*, **6**, 8854, doi:10.1038/ncomms9854.
- Unisys, 2015: Hurricane tropical data. *Unisys weather*. [Available at <http://weather.unisys.com/hurricanes/>.]
- Wang, B., and J. C. L. Chan, 2002: How strong ENSO events affect tropical storm activity over the western North Pacific. *J. Climate*, **15**, 1643–1658.
- Wang, B., R. Wu, and X. Fu, 2000: Pacific–East Asian teleconnection: How does ENSO affect East Asian climate? *J. Climate*, **13**, 1517–1536.
- Wang, B., Q. Ding, X. Fu, I.-S. Kang, K. Jin, J. Shukla, and F. Doblas-Reyes, 2005: Fundamental challenge in simulation and prediction of summer monsoon rainfall. *Geophys. Res. Lett.*, **32**, L15711, doi:10.1029/2005GL022734.
- Wang, B., J. Li, and Q. He, 2017: Variable and robust East Asian monsoon rainfall response to El Niño over the past 60 years (1957–2016). *Adv. Atmos. Sci.*, **34**, 1235–1248.
- Webster, P. J., G. J. Holland, J. A. Curry, and H.-R. Chang, 2005: Changes in tropical cyclone number, duration, and intensity in a warming environment. *Science*, **309**, 1844–1846.
- Wu, C.-C., R. Zhan, Y. Lu, and Y. Wang, 2012: Internal variability of the dynamically downscaled tropical cyclone activity over the western North Pacific by the IPRC regional atmospheric model. *J. Climate*, **25**, 2104–2122.
- Xie, S.-P., H. Annamalai, F. A. Schott, and J. P. McCreary, Jr., 2002: Structure and mechanisms of South Indian Ocean climate variability. *J. Climate*, **15**, 864–878.
- Xie, S.-P., K. Hu, J. Hafner, H. Tokinaga, Y. Du, G. Huang, and T. Sampe, 2009: Indian Ocean capacitor effect on Indo-western Pacific climate during the summer following El Niño. *J. Climate*, **22**, 730–747.
- Xie, S.-P., Y. Kosaka, Y. Du, K. Hu, J. S. Chowdary, and G. Huang, 2016: Indo-western Pacific Ocean capacitor and coherent climate anomalies in post-ENSO summer: A review. *Adv. Atmos. Sci.*, **33**, 411–432.
- Yoshida, K., M. Sugi, R. Mizuta, H. Murakami, and M. Ishii, 2017: Future changes in tropical cyclone activity in high-resolution large-ensemble simulations. *Geophys. Res. Lett.*, **44**, 9910–9917.
- Zhan, R., Y. Wang, and X. Lei, 2011a: Contributions of ENSO and east Indian Ocean SSTA to the interannual variability of northwest Pacific tropical cyclone frequency. *J. Climate*, **24**, 509–521.
- Zhan, R., Y. Wang, and C.-C. Wu, 2011b: Impact of SSTA in the East Indian Ocean on the frequency of Northwest Pacific tropical cyclones: A regional atmospheric model study. *J. Climate*, **24**, 6227–6242.
- Zhan, R., Y. Wang, and M. Wen, 2013: The SST gradient between the southwestern Pacific and the western Pacific warm pool – A new factor controlling the Northwest Pacific tropical cyclone genesis frequency. *J. Climate*, **26**, 2408–2415.
- Zhan, R., Y. Wang, and L. Tao, 2014: Intensified impact of East Indian Ocean SST anomaly on tropical cyclone genesis frequency over the western North Pacific. *J. Climate*, **27**, 8724–8739.
- Zhang, Q., L. Wu, and Q. Liu, 2009: Tropical cyclone damages in China 1983–2006. *Bull. Amer. Meteor. Soc.*, **90**, 489–495.